Determination of the single-molecule position and orientation

Gloria Micó Cabanes

University of Groningen

September 2010 – February 2011

INDEX

1. INTRODUCTION

Fluorescence consists in the emission of a photon from a molecule, called fluorescent molecule, due to a previous optical excitation. Fluorescence microscopy is an imaging technique in which the sample we want to study is itself the light source because emitting fluorescence. If the sample does not emit light by itself, it can be labelled with a fluorophore, which is a fluorescence molecule.

Fluorescence-based techniques are valuable tools for studying cellular structure and functions, and also the interactions between molecules in biological systems. Fluorescence-based approach is the most rapidly expanding microscopy technique employed today. This has spurred the development of more sophisticated microscopes (such as epifluorescence, confocal or total internal reflection fluorescence microscopes) and numerous fluorescence sources (fluorescent proteins, fluorescent stains).

The need for further study the cellular sub-structures triggered the development of new techniques with high resolving power as Super Resolution Microscopy (SRM). With this technique we are able to achieve deeper characterization of the investigated specimens. SRM is explained in more detail in section 2. Single molecule studies remove ensemble averaging, characteristic of bulk measurements, and can provide information on the behaviour of individual molecules[1]. A topic of special interest has always been the experimental determination of the position and orientation of single molecules since photophysical parameters of single molecules such as fluorescence lifetime and observable emission intensity often depend on the orientation of the molecules.

So far, people who work in this topic use different approaches to get information about the position and the orientation: i) Focus imaging and ii) Defocus imaging and iii) Emission polarization analysis. By exploiting the theoretical knowledge of the spatial distribution of photons in the image, the focus imaging method provides high accuracy concerning the determination of the position of the molecule. Still it cannot get any information about the orientation of the molecules. On the contrary, with defocus imaging, the orientation of the molecules can be determined, but, because of the lower signal-to-noise, the accuracy in the measurement of the position is poorer. In many published articles on the Single Molecule Microscopy, these two approaches are mostly used to acquire the desired information[2,3,4,5]. The third one (emission polarization analysis[6,7]) provides a better determination of the orientation than defocus imaging technique, but the information obtained with the second approach is precise enough for this experiment. Thus orientation and position (with high accuracy) information can not be obtained at once. This is the essence of the problem: to resolve position and orientation, it is necessary to take two different images (focus and defocus images) which increases the experimental difficulties and limits the temporal sensitivity.

The main goal of this project is to propose a novel and possibly better solution. Our results support the possibility to measure both the position and the orientation of the molecules while imaging the molecules in the focal position (focus imaging). This enables to maintain the high accuracy in the position measurement and, at the same time, to obtain the information about the orientation of the molecule. Detailed explanation of this approach is discussed in section 2.2.

1.1. Theoretical Concepts

1.1.1. Fluorescence

Fluorescence is a photophysical process that defines the property of some atoms and molecules to absorb light at a particular wavelength and subsequently to emit light at longer wavelength. A fluorophore is a component of molecules which causes the molecule to be fluorescent. The main characteristics of a fluorophore are i) the fluorescence lifetime, that refers to the average time the molecule stays in its excite state before emitting a photon and ii) the quantum yield, that is the number of emitted photons relative to the number of absorbed photons.

The energy level structure of a molecule can be represented with a Jablonski Diagram where the different electronic states and vibrational levels of the molecule are shown (Figure 1.1). In the ground state, the fluorescent molecule is in a relative laid low energy stable configuration and it is not fluorescent. When light from an external source hits the fluorescent molecule, the molecule can absorb the light energy and the electron in the electronic ground-state level goes to a higher vibrational level of the excited state. This electron decays quickly to the lowest vibrational level. This process is known as internal conversion and the range of time of this process (lifetime) is between 10^{-15} and 10^{-9} seconds[8]. Then, the electron returns to the ground state emitting a photon, what is called fluorescence. Once back in the ground state, the fluorophore can absorb light energy again and go to the entire process repeatedly.

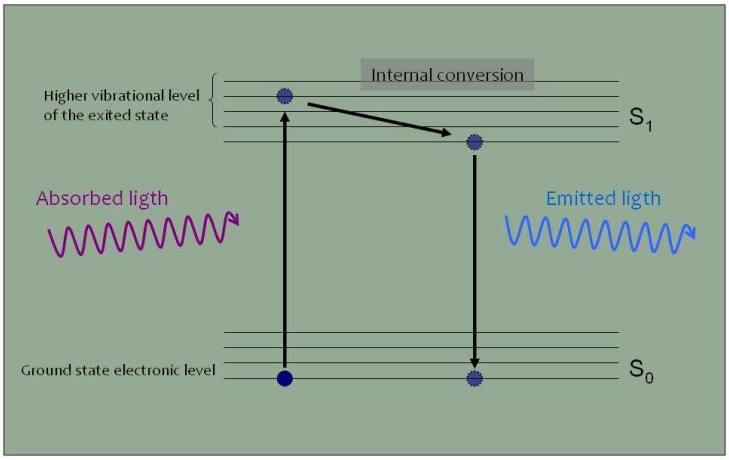

Figure 1.1. *Jablonski diagram where is shown a schematic representation of the process to get fluorescence.*

Examination of the Jablonski diagram reveals that the energy of the emitted light is normally lower than the energy of the absorbed light. In other words, the wavelength of the fluorescence emission is longer than the wavelength of the absorbed light. This is because of the loss of energy in the internal conversion. The process is known as Stokes shift.

The number of fluorescence cycles is though limited by photobleaching. This photophysical process occurs when a fluorophore permanently loses the ability to emit fluorescence due to photon-induced chemical damage and covalent modification. The average number of excitation and emission cycles that occur for a particular fluorophore before photobleaching is characterized by the molecular structure and the local environment. Furthermore, there is the possibility that specimen can lose its excitation by nonradiative processes such as collisions with other atoms or molecules. This is known as quenching.

1.1.2. Fluorescence and single molecules microscopy.

The technique of fluorescence microscopy has become an essential tool in biology and biomedical sciences, as well as in materials science thanks to the attributes that are not readily available in other contrast modes since fluorescence microscopy is an extremely sensitive method, allowing the detection of single molecules. For example, the application of an array of fluorochromes has made it possible to identify cells and sub microscopic cellular components with a high degree of specificity amid non-fluorescing material. Using fluorescence microscopy, the precise location of intracellular components labelled with specific fluorophores can be monitored, as well as their associated diffusion coefficients, transport characteristics, and interactions with other biomolecules[9]. Through the use of multiple fluorescent labels, different probes can identify simultaneously several target molecules.

The ultimate goal in ultra-sensitive detection schemes is the observation and characterization of the investigated system at the single molecule level. The need for such techniques emerges from analytical chemistry on one hand and from physical and biological sciences on the other hand[10]. Studies performed at the level of individual molecules can resolve subtle effects which are hidden in the ensemble-averaged signals obtained from experiments using bulk solutions.

2. METHOD

2.1. Super Resolution Microscopy (SRM)

The optical resolution limit imposed by light diffraction has always been a major obstacle in imaging techniques since preventing the access to insights of the fabric of living cells. The limited resolution of fluorescence microscopy leaves unresolved many biological structures too small to be studied in detail (light is a wave and the microscope runs into trouble when the distance between objects of interest is less than half the wavelength of the light). In 1990s, scientist realized they could go beyond the diffraction limit. When this happened, the field of super-resolution light microscopy took off.

To understand how they bypassed this law, we must first understand the meaning of a crucial element in microscopy or any imaging technique: the Point Spread Function (PSF). PSF describes the response of an imaging system to a point-like source, that is a source of light which physical size is much smaller (one or two order of magnitude) than the wavelength of the emitted light. The relevance of the PSF is central since it coincides with the optical resolution of the microscope. As the name suggests (Point Spread Function), the image of a point is spread over a wider area because of light diffraction. This generates a fundamental limit to the resolution power: we can not see details smaller than the size of the PSF.

Mathematically, PSF is described by the Airy function (Figure 2.1). Airy studied the diffraction limited distribution of photons from a circular aperture. To get his solution he made two assumptions: 1) the light is unpolarized and 2) the collection angle is very small (paraxial approximation). The collection angle is defined as the apparent angle of the lens aperture as seen from the focal point.

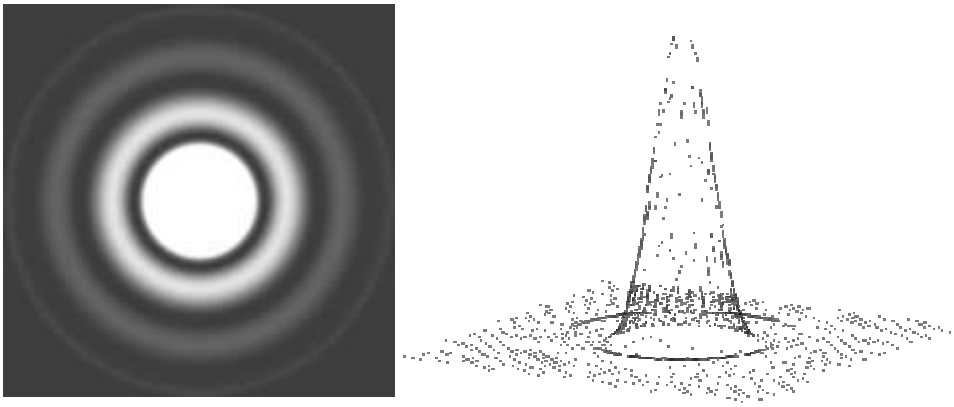

Figure 2.1. *Airy pattern in 2D and 3D. The central disk is known as Airy Disk and contains about the 80% of the total intensity of the pattern.*

Until 1990s (classical microscopy), the details level we could achieve had the size of the PSF. This was a problem in biology since this resolving power was not enough to study smaller structures. This has boosted the "development" of what is known as Super Resolution Microscopy.

Super Resolution Microscopy (SRM) uses the information that there is in a single molecule within the PSF area and determines (with one or two higher order of magnitude) its central position with accuracy beyond the diffraction limit. One graphic example of this is shown in the figure 2.2. The goal of this example is to determine the position of a single molecule (represented by the red spot) which size is about 1nm, its emission wavelength is 520 nm and the optical resolution is about 230 nm. In classical microscopy the details level we can achieve has about the size of the PSF. We cannot achieve details much smaller than the PSF.

Nevertheless, when the Airy function is used to model the PSF, the position of the molecule can be determined with accuracy between 1 and 2 nm. The formula used to calculate the limit of the measureable accuracy is found in the references[11] and it depends on the standard deviation of the PSF, the pixel size, the background noise (which occurs when detected photons do not necessarily originate from the molecule) and the number of photons collected.

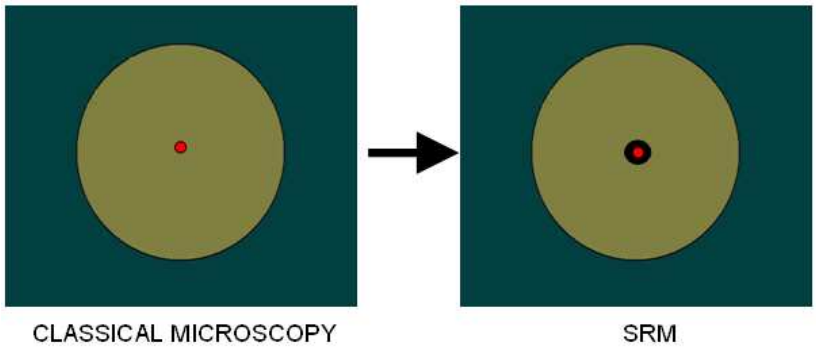

Figure 2.2. *Graphic scheme of the measurement accuracy of the position of a molecule with Classical Microscopy and Super Resolution Microscopy. The PSF is represented by the big green circle, the molecule is the small red spot and the accuracy in SRM is drawn as the black circle surrounding the molecule.*

So far, we discovered how is possible to determine the position of a single molecule with accuracy beyond the diffraction limit, still the information about the orientation of the molecules is completely missing.

2.2. One step further (Theoretical model)

In 1959, E. Wolf and B. Richards[12] modelled the PSF by solving the diffraction problem without the two assumptions Airy used. Their results show the dependence of the PSF symmetry on the collection angle in case of polarized emitter. In the simulations of figure 2.3, it is shown how the shape of the PSF becomes elliptical when increasing the collection angle (α). In the simulation, the light polarization remains along the horizontal direction as shown by the arrows.

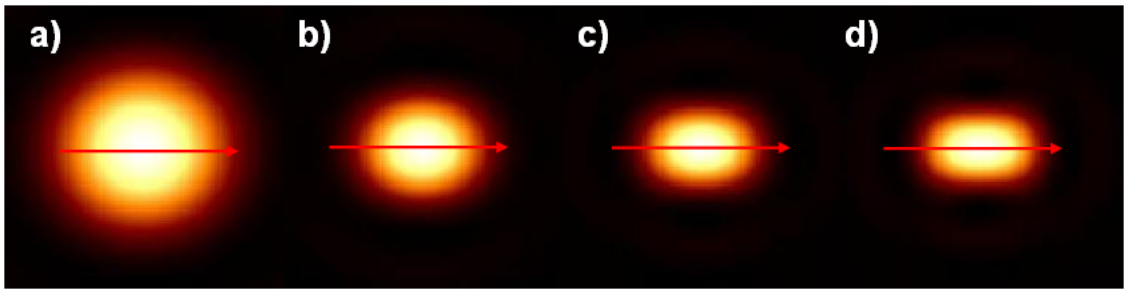

***Figure 2.3**. PSF dependence on the collection angle. The collection angle in each case is a) $\alpha = 30^{o}$, b) $\alpha = 50^{o}$, c) $\alpha = 70^{o}$ and d) $\alpha \rightarrow 90^{o}$. When $\alpha \rightarrow 0^{o}$ the figure is identical with the classical intensity pattern of Airy showed in the figure2.1.*

PSF changes form circular to elliptical shape and elongates along the direction of the dipole, i.e. the long axis of the ellipse coincide with the axis of the dipole. Knowing this, the orientation of the dipole can be evaluated by measuring the orientation of the long axis of the elliptical PSF.

It is important to remark the two conditions taken into account in arriving at this solution: 1) the emitted light from the light source is linearly polarized and 2) the collection angle of the system has to be big enough to observe the elliptical shape of the PSF.

Modern microscopy allows us to move from theory to experiment, meaning we are able to recreate these conditions. Nowadays, it is possible to use objective providing a high collection angle; in our experiment is about 70º (figure 2.3c). To get polarized light we have to work on the sample we want to study. It will be explained in section 2.5. Satisfied the two points, we are able to recreate experimentally the conditions assume for the theoretical model.

As mentioned earlier, the main goal of this thesis is to achieve detailed characterization of the position and orientation of a single fluorescent emitter and the proposed method exploits the following idea. The in-focus imaging of elliptical PSFs provides us accurate information about the position and orientation of the molecule.

2.3. Experimental setup

The most important apparatus of the optical setup is the optical microscope. It is called fluorescence microscope because fluorescence is used on it. To explain how it works we will build on the graphic scheme showed in the figure 2.4. The excitation light from the laser (488 nm line from Ar^+ laser) is reflected towards the sample by the dichroic mirror, used to separate the laser illumination from the fluorescent emission. As it has been explained above, some fluorophores can absorb this light and they emit light of longer wavelength. This light passes through the dichroic mirror and then through the Notch filter. This is a specific filter that transmits most frequencies, but stops those in a specific narrow band (in this case around 488 nm). Finally, the emitted light of the molecules goes into the detector (CCD camera).

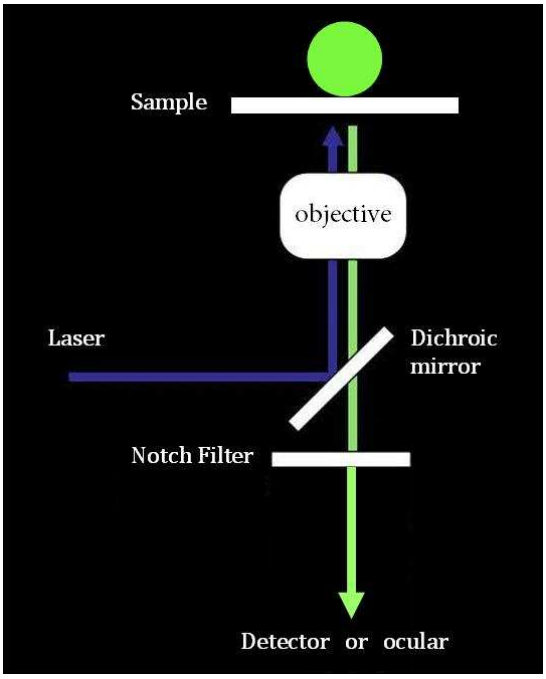

Figure 2.4. *Schematic of a fluorescence microscope.*

To achieve a more homogeneous excitation profile (Gaussian) on the illuminated area, the laser beam is made broader by the use of a telescope. The intensity distribution achieved has a difference of 10% between the centre and the edges of the illuminated area.

The objective used in the microscope magnifies the object and collect the photons from the sample. This one is an oil immersion objective. This means that between the microscope coverslide, on which is the sample, and the objective there is a thin film of oil that improves the resolving power by a factor 1/n, where n is the oil refraction index. With this kind of objective the Numerical Aperture (NA) (dimensionless number that tells us the value of the collecting angle over which the objective can collect light) is significantly increased. The NA is defined mathematically by $NA = n\sin(\alpha)$, where α is the collection angle. The value of the NA is 1.4 in our experiment, considering that the refraction index of oil is 1.52, the resulting collection angle is 70º.

Figure 2.5 represents the curve of the ellipticity (value which measures how much the ellipse deviates from being circular) obtained for each value of the NA (collecting angle) obtained through simulations and the experimental value. The experimental point is close to the theoretical curve. The ellipticity is calculated as $e = \sqrt{1 - \left(FWHM_Y / FWHM_X \right)^2}$. The experimental point is the best one obtained (Section 4).

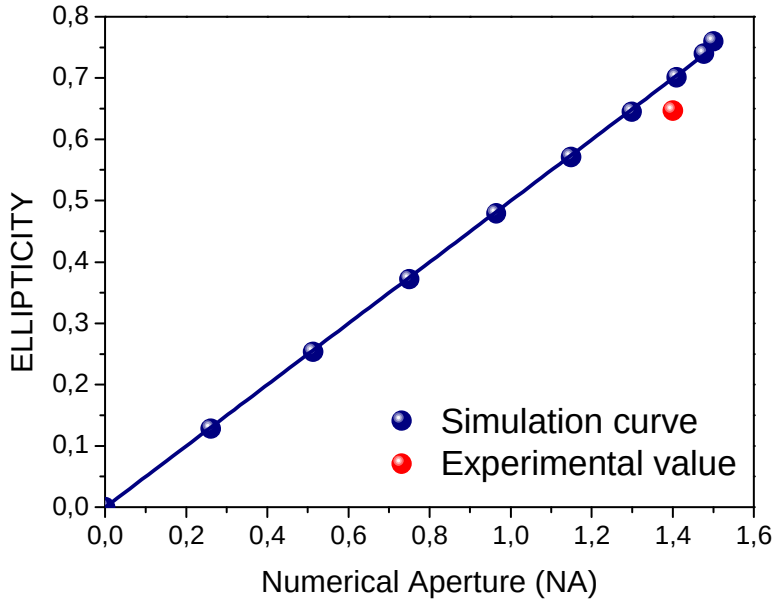

Figure 2.5 *Visual comparison of the ellipticity obtained in our experiment and that obtained through simulations.*

Alexa Fluor 488 molecules are used in the experiment because of their high quantum efficiency (~95%) at 488 nm resulting in very bright fluorescence sources. To fix these molecules a polymer matrix (PMMA) is used. A further explanation about the sample and its preparation is done in the section 2.5.

Pictures of the complete experimental setup are shown in the Annex with more details.

2.4. Cleaning procedure

To work effectively with single molecules all the utensils used must be properly decontaminated to be sure that the molecules observed in the sample are the molecules we want to study.

The first step in the cleaning procedure is to sonicate the glass slides in 2% Hellmanex (detergent-mix) for one hour at 60ºC in a sonication bath. After this, each slide must be washed three times with MQ water. The next step is to sonicate again the slides in MQ water for 30 minutes at 60ºC. Once again, the slides will be washed three times with MQ water. Following this, 1 hour sonication in 1M KOH (also at 60ºC). This step also improves the wetting property of the glass surface (no drop formation). To finish, after washing again the slides three times in MQ water, they were dried quickly with air.

The slides used in this experiment are from Menzel. These slides are made of glass and their thickness is 0.17 mm designed for the working distance of the objective. It is known that the coating for some plastics is fluorescent and get dissolved in organic solvents for this reason no plastic bottles or tubes were used.

2.5. Sample preparation

The sample must satisfy two different requirements: 1) the concentration of molecules has to be low enough to distinguish each individual single molecule, and 2) the emitted light has to be polarized to observe the elliptical shape of the PSF of each molecule.

To get polarized light, molecules have to be fixed in the sample. A polymer matrix is used for that. Polymethyl methacrylate, which is abbreviated as PMMA, is a clear plastic used as a shatterproof replacement for glass. The glass transition temperature of PMMA ranges from 85 to 165ºC, which means at room temperature the PMMA has glassy properties.

To start the sample preparation two different solutions are needed: highly diluted Alexa Fluor 488 in Chloroform and PMMA in Chloroform. For the second solution, 10 mg of PMMA were added to 10 ml of Chloroform, and the solution was put on a rotating magnetic field stage with a stirring bar for 45 minutes to dissolve completely the polymer.

The sample has a composition 1/8 of Alexa and PMMA concentration, this means, the amount of PMMA and Chloroform it will be eight times greater than Alexa Fluor and Chloroform. This is the best ratio of solutions for the sample as with less amount of PMMA the molecules are not fixed and with more amount of Alexa Fluor the concentration to observe single molecules is too high.

After preparing the solution, one of the clean slides is put in the spin coating device and two drops of the final solution are deposited in it. The time of the sample in the spin coating is around 1 minute. With this procedure we get a thin film (~ 100 nm) of our sample which is significantly important. If the thickness of the sample is too large, molecules will not be in the same plane and because of this, the focus measurements will not be correct. When the spin coating is finish, the sample is covered with a glass slide for the microscope and it is ready to measure it.

2.6. Measurements

In our experiment, we performed two different measurements: focus and defocus imaging. As it was explained in section 2.2, focus imaging provides high accuracy for the position, and defocus imaging for the orientation. We want to compare the orientation measurements done while in focus (exploiting the elliptical shape of the PSF) to the defocus approach. To have direct comparison between the angle's value measured in focus (new) and defocus (old) the same molecules must be imaged with both the approaches.

The first step is to find the correct focal position. This process has to be done carefully. Pictures shown in figure 2.5 are an example of the correct and wrong focal position. The wings that appear in the figure 2.5b) are due to the emission pattern of the molecule when it is imaged lightly (~100-200 nm) defocused (it will be further explained). If a picture as 2.5b is fitted with the computer programme, the molecule will be consider as the collection of the own molecules and the wings, and the data obtained

will be incorrect. If the image of the molecule is too defocused, the elliptical shape fitted by the programme can result 90° rotated respect the correct value.

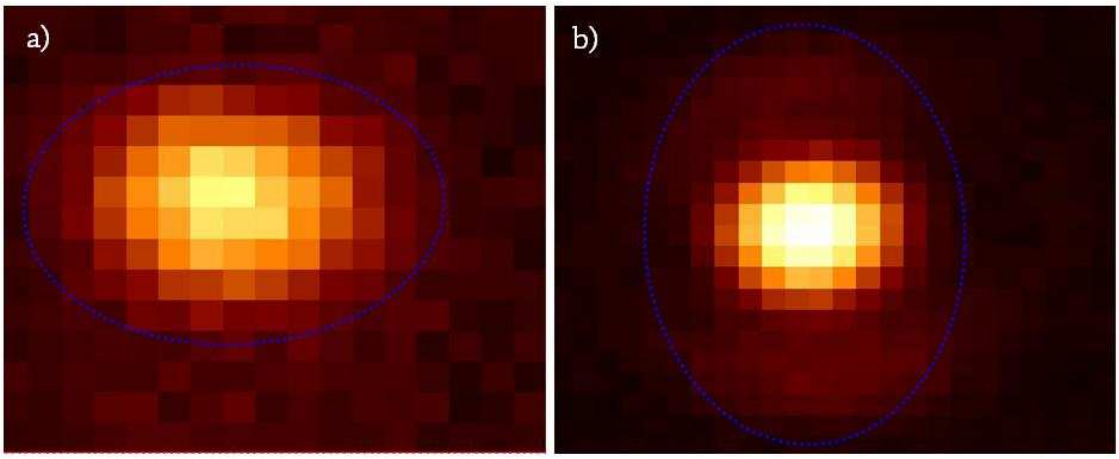

Figure 2.5. *Focus imaging. a) Molecule imagined in the focal position. b) Molecule imagined in a shifted focal position. The blue ellipses provide us an approximate idea about the fit of the molecules after being analysed by the program.*

To get defocus images, the sample is shifted (1 μm) above the focal position. In this case, the object observed is the emission pattern of our molecular dipole, which is shown in the figure 2.6a). The defocus imaging of a single molecule assumes such pattern because its emission is the same as of an electric dipole. A single fluorescing molecule is a single emitting dipole. In figure 2.6b) is shown the emission pattern of an electric dipole in two and three dimensions. The 3D pattern resembles the emission of a dipole oriented along the vertical axis. When this pattern is observed in a parallel plane to the vertical direction, as in figure 2.6 and in the 2.6 b (2D), it will provide the orientation of the dipole.

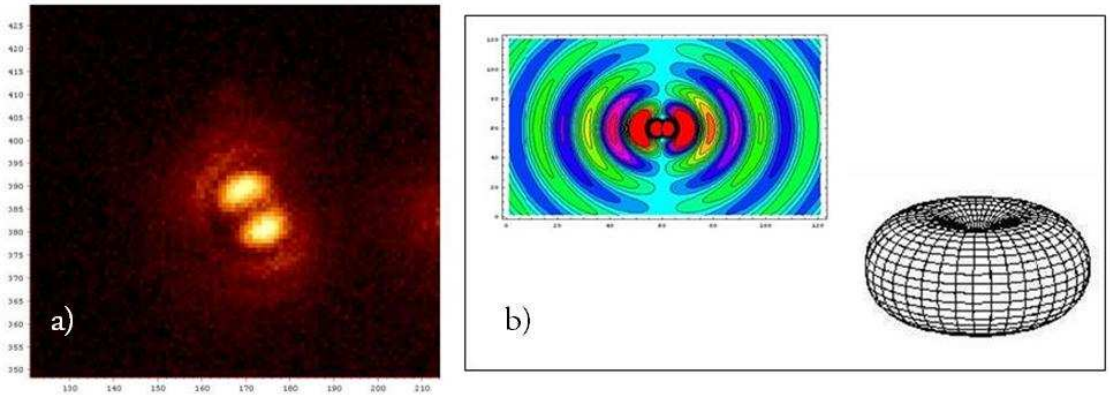

Figure 2.6. a) *Emission pattern of a single molecule,* ***b)*** *emission pattern of an electric dipole in 2 and 3 dimensions.*

In reference to figure 2.5b, it's now easy to understand why the wings appear. When the focal position is not the correct one, the emission dipole pattern of the molecule becomes visible mildly and the wings can be observed.

The experiment consists of first to get images of the sample in the focal position. The exposure time in this position is 0.5 s. After this time, the laser beam is blocked to avoid the photobleaching and the sample is shifted to a defocal position 1 μm above the focal one. Once the sample is in the new position, the laser beam is open and image with exposure time of 1.5 s is collected. Obviously, the area illuminated in both positions is the same because the goal of these measures is to compare the values obtained for each one. The light used to excite the molecules is circular polarized light (to excite homogeneously all the randomly oriented molecules) and the power density is $200 W/cm^2$.

The main problem in these measurements is the photobleaching. We have to be fast to find the correct focal position, otherwise when we try to image the molecules in a defocal position, they will be gone because of this.

Once pictures are taken, the next step is to analyze them. A two dimensional Gaussian function with two independent values for orthogonal axis (long and short in case of elliptical shape) and with term related to the orientation of the long axis was used to model the PSFs. So, the analysis of the imaged PSFs provides us position, angle, amplitude, full width half maximum (FWHM) of the major and minor axis, and the ratio between them. The results obtained are discussed in the next session.

3. RESULTS AND DISCUSSION.

3.1. Focus-defocus correlation.

The analysis shows the Full Width Half Maximum (FWHM) distribution of the major and minor axis of the ellipse (Fig. 3.1). The FWHM is related with the standard deviation of the PSF (σ) according to:

$$\sigma = \frac{FWHM}{2\sqrt{2\ln 2}}$$

In this way we can see the distribution of size of both axes and obtain the ratio between them (red curve in figure 3.2), which is about 1.2. Ratio between both axes and the ellipticity are related as $r = \frac{1}{\sqrt{1-e^2}}$. As it was said in section 2.3, in our experiment the NA is 1.4. From the blue curve of the figure 2.3 we can obtain the value of the ellipticity for this NA and then calculate the ratio. So, theory tells us the ideal value of the ratio is 1.35, but this number is hard to obtain due to the difficulty to find the correct focal position when the measurements are made.

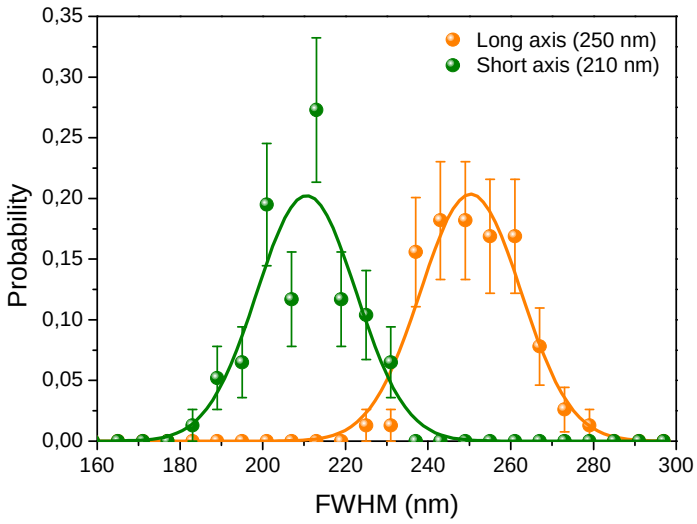

Figure 3.1. *FWHM distribution graph of the major and minor axes of the PSF.*

Still in figure 3.2 it is represented the correlation between FWHM of the major and minor axis of the same molecule. The goal of this fit is to observe if the behaviour of the data is random or they follow a commune pattern. As we see in the figure, the slope value of the correlation is the inverse of the ratio. This demonstrates that the analyses are done correctly.

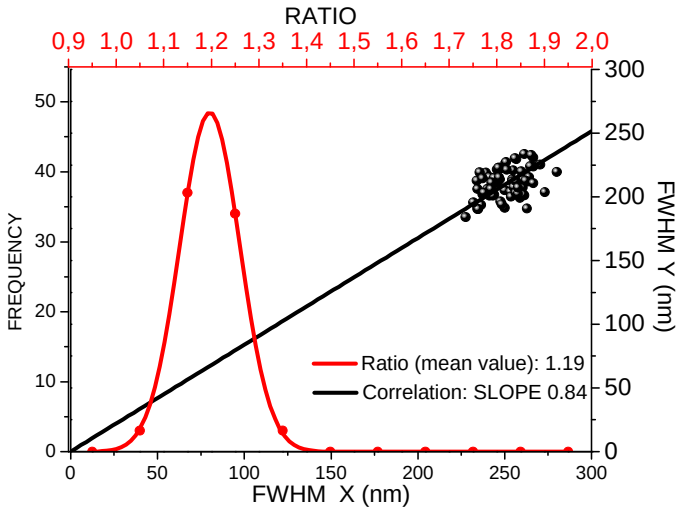

Figure 3.2. *Ratio distribution graph combined with the correlation between the FWHM of the major and minor axis of the PSF.*

The third graph showed below (figure 3.3) represents the intensity distribution of the light from the imaged molecules. The intensity is calculated with the data obtained as:

$$I = 2\pi\sigma_X\sigma_Y H$$

where σ_X, σ_Y are the standard deviation of the major and minor axis of the PSF respectively and H is the amount of photons collected. The intensity distribution shows the molecules to emit significantly high number of photons due to high quantum yield of the fluorescent molecules and to rather long integration time (0.5s). This was done since interested in the proof of principle. We are confident the same analysis can be achieved with lower photon count.

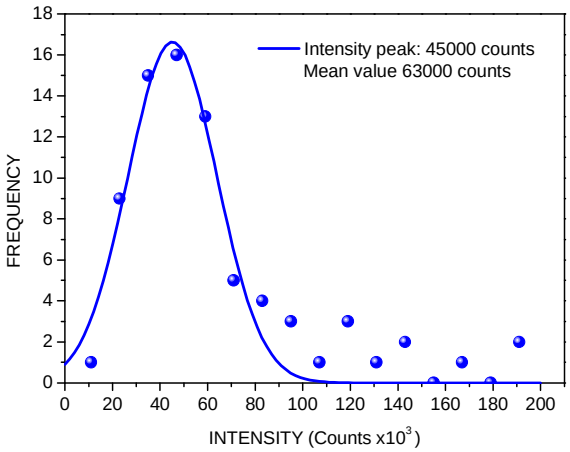

Figure 3.3. *Intensity distribution graph.*

The analysis concerning the FWHM of the two axes of the PSFs clearly support the achieved elliptical shape. Still, the main goal of these analyses is to measure the orientation of the molecule and compare the obtained value with the defocus imaging approach. The data obtained for the angle with both experiments are represented in a correlation graph (figure 3.4.). In the X axis has been represented the value of the angle obtained with the focus approach and in the Y axis the one got with the defocus approach.

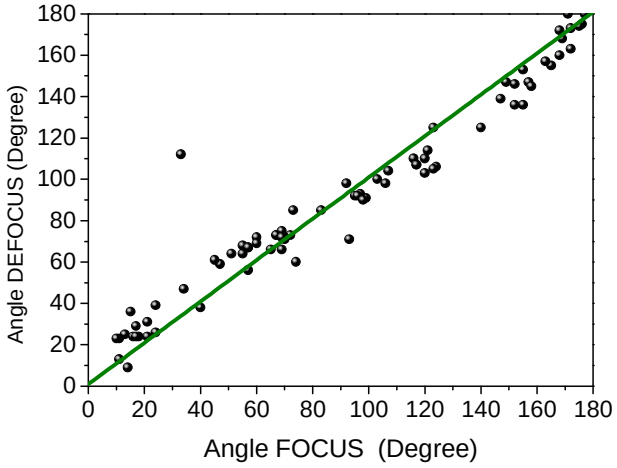

Figure 3.4. *Focus-defocus angle correlation.*

The green line represents the ideal value correlation. The distribution of the points significantly follows the ideal case. The divergence in value is about 13 degrees, value that represents the error done with the new approach.

As you can observe in the figure, there is a deviation in the distribution but only in some intervals of values ((45 ± 15) º and the complementary angle (135 ± 15) º). This deviation resembles a sort of modulation in the focus values that can be due to the two prisms inside the microscope. Further and more careful analysis has revealed that modulation due to these prisms and the compensation of their effect has greatly improved the correlation of focus/defocus. Now, the accuracy associated with our measures is around 5 degrees.

The number of studied molecules in this analysis is about 80. This amount is good enough to get correct results because, previously, there were other tests and we found that it was better to study molecules with greater intensity emission. For these other analyses the amount of studied molecules was about 5000 molecules. A further explanation of these first experiments it will be done in the section B of the annex.

3.2. Dependence accuracy on the pixel size.

The first thought after obtain these results was how could we improve them and for that we went back to the theory. In the section 2.1 (SRM) was discussed the employed expression to calculate the error of the position of a single molecule[2]. This expression is a set of different errors coming from several kinds of noises. Background noise occurs when detected photons are not necessarily originated from molecule being studied. Photon noise is due to the photons from the particle being localized. Each photon collected in the image gives a measure of the position of the object and the best estimate of the position is given by the average of the positions of the individual detected photons. The last one is the pixelation noise. This noise is due to the finite size of the pixel and the uncertainty of where the photon arrived in it. The apparent size of the molecule is influenced by the pixel noise; this can also influence the accuracy in the determination of the molecule's orientation.

During the experiment, we found some problems with the pixel size in two different extreme cases. When a molecule image is placed in a single pixel (big pixel sizes), there is no ellipticity as the pixel is square. So as the pixel size becomes bigger, the accuracy decreases. The other extreme case is the opposite: small pixel sizes. In this case, a fixed amount of photons is dispersed amongst many more pixels. Therefore, the number of photons per pixel decreases and the CCD noise become important thereby the accuracy diminished again. Then, of both the big and small pixel size are bad. There is an optimum size, but it depends on the particular experimental conditions. For most situations, this optimum pixel size would be around 80 nm in which is a bit smaller than for the localization microscopy.

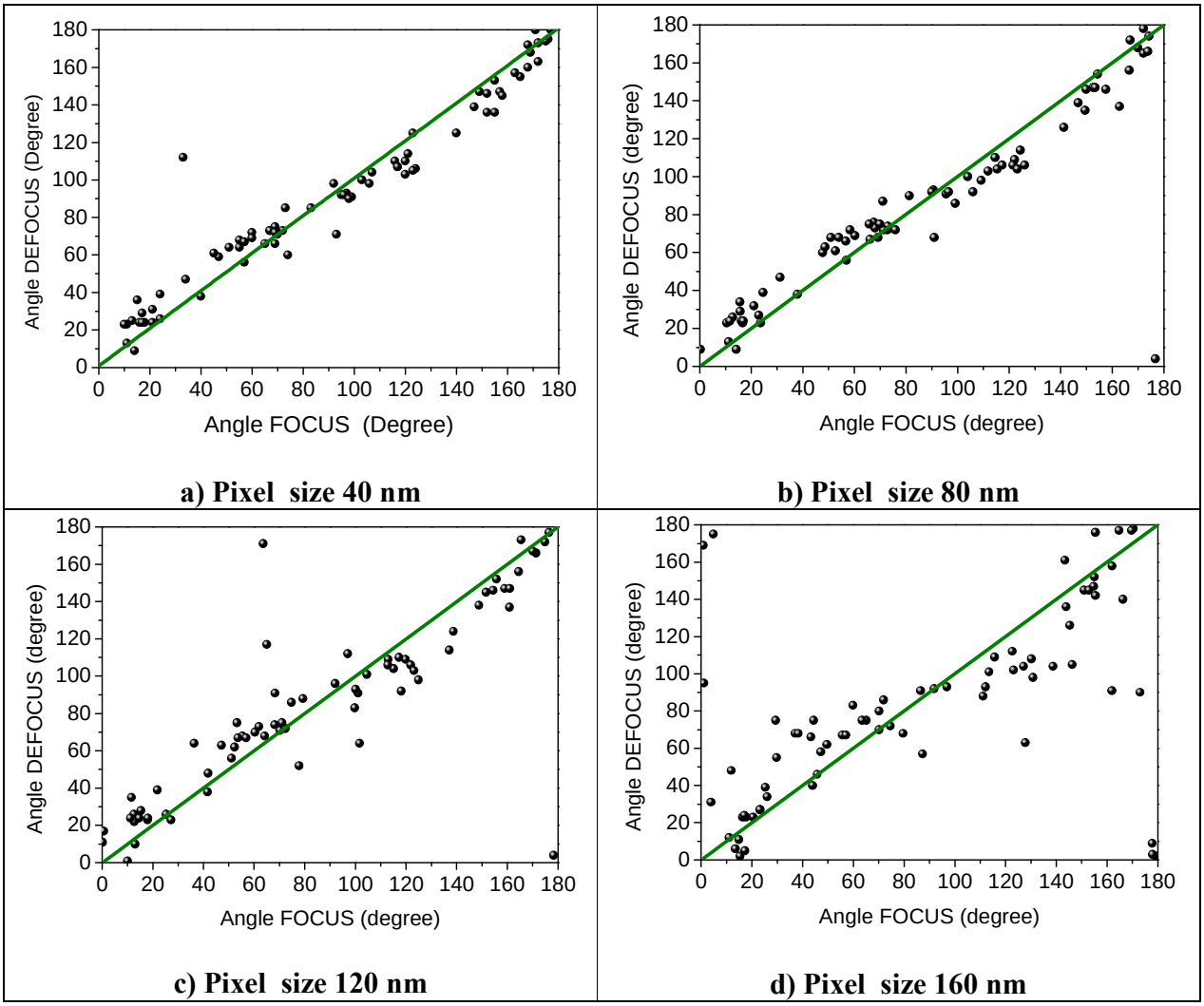

Figure 3.5. *Correlation distribution for a) 40 nm pixel size, b) 80 nm pixel size, c) 120 nm pixel size and d) 160 nm pixel size.*

Experimentally, to get different sizes of pixels the best option was to change the objective (or the total magnification) of the microscope and take images with diverse graduations. This was not possible. We partially solved the problem by using software to group the pixels (binning). This program takes the analyzed pictures with a pixel size of 40 nm (image pixel size) and then it puts the pixels into groups of 2, 3 or 4 pixels depending on the chosen option. In this way the pixel size is 80, 120 or 160 nm respectively.

The first observation we can make about these graphs is the distribution of the points along the ideal line. When the pixel size increases, the dispersion of the points along this line increases too. This is due to the fact that the molecules are defined with lower number of pixels and the determination of the angle is not completely correct. As it

is shown in the figure below, when the pixel size is too large it is almost impossible to fit the shape of the molecule.

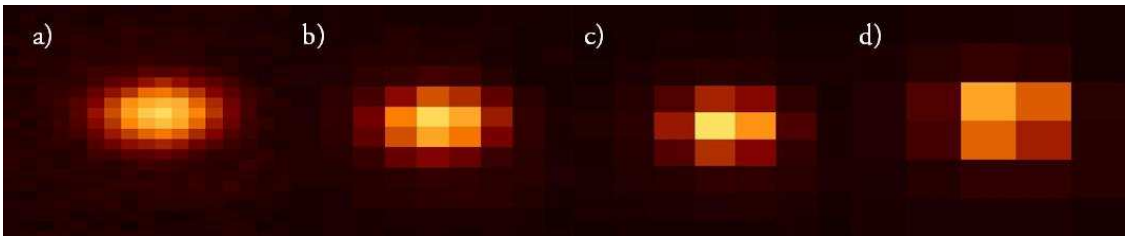

Figure 3.6. *Image of a molecule depending on the pixel size. a) 40 nm, b) 80 nm, c) 120 nm and d) 160 nm.*

There is a parameter which decreases with the pixel size: the ratio between the axes of the FWHM. In the previous section it said the ratio for 40nm pixel size was 1.19. The analyses of these data show that the values of the ratio are 1.18, 1.14 and 1.11 for 80, 120 and 160 nm pixel size respectively. This value is getting worst (it should be close to 1.35) due to the difficulty of the program to fit the correct shape of the PSF of the molecules.

The figure 3.7 represents the different angle accuracy value for each pixel size. In this grahp, the number of photons analysed is 5000 and the CCD noise is about 150.

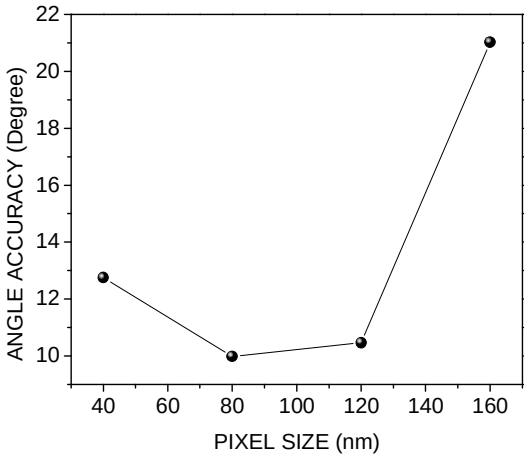

Figure 3.7. *Graph of the angle accuracy.*

As we can see, the precision in the measure of the angle is much better for 80 or 120 nm than for 40 nm pixel size. For 80 nm the angle accuracy is 10º and for 120nm is 10.5º. In this point we have to choose the best option to image our molecules. If we consider all the results obtained for each pixel size, the best option is 80 nm because, firstly, it has the best angle accuracy and secondly, the dispersion of the data along the ideal line is low enough to take these values as compatible. As it was said in the previous section, angle accuracy improves when modulation of the two prisms is taken in account.

4. APPLICATION EXPERIMENT.

To prove if our approach works properly, we thought in an application experiment which consists of check the behaviour of Alexa molecules and the growth of the PMMA thin film when in presence of pre-oriented structures such as stretched PTFE molecules[13].

PTFE is a synthetic fluoropolymer of tetrafluoroethylene generally known as Teflon. When a surface is scratched with a Teflon bar along a determined direction, PTFE molecules are adsorbed onto the glass surface by frictional force and follow the orientation of the scratching direction. It is speculated that the presence of such long and pre-oriented molecules on a smooth surface might drive the grown of material following the direction of the PTFE molecules.

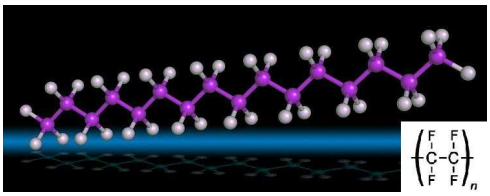

***Figure 4.1**. Structure of PTFE molecules.*

The preparation of the sample followed these steps. First, the coverslide were scratched with a Teflon bar along their long axis. To ensure that this action was correct, several samples were made changing the strength and the number of the scratches (10 was the optimal number). Second, a solution containing Alexa Fluor 488 and PMMA in chloroform was spin coated onto the 'pre-functionalized' surface. In details: 5ml of chloroform solution with PMMA (12 mg PMMA in 10 ml chloroform) and 1 ml of chloroform with Alexa molecules.

The obtained samples were then imaged in movies of 100 frames at 2 Hz. With this we get to remove some molecules because of the photobleaching and therefore molecules can be analyzed in a better way, as the disadvantage of these measures is the high concentration of molecules. Could we decrease this concentration during the sample preparation? The answer is affirmative, but then obtaining the images is more complicated as adjusting the focal position and start to measure the molecules being analyzed will be destroyed. Several movies were taken displaying different areas of the sample. After this, the movies were analyzed.

To improve that analysis and to achieve consistent representation of the samples, not all of the frames displayed in the movies were analyzed. In particular we focus our attention on frames from 5th to the 15th. This was done for two reasons: first the too high Alexa concentration prevented a clear analysis of single emitters and because of that we take advantage of photobleaching in order to get a suitable concentration. Second, a slightly displacement of the sample prevented the molecules to be in the proper focal position throughout the entire movies.

Analysis of imaged molecules provides a statistical representation achieved by considering each single molecule only once. The total number of analyzed molecules is 85.

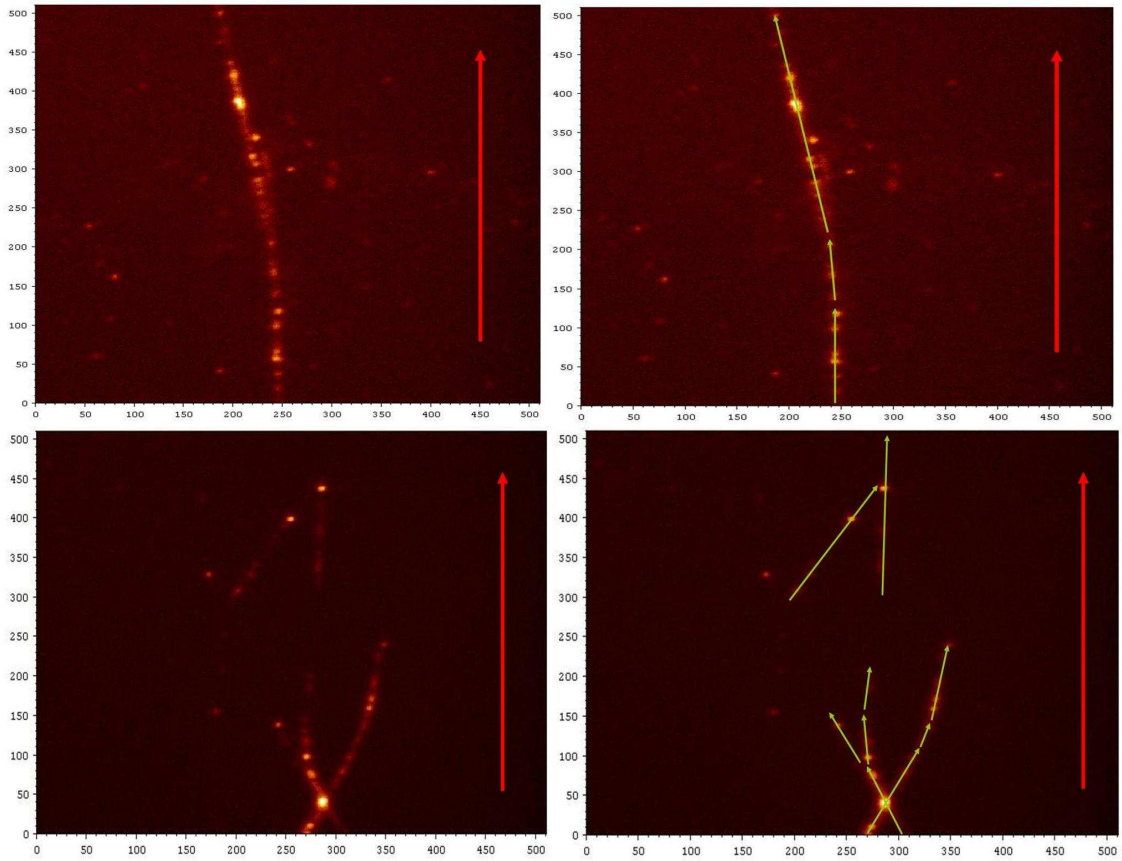

Figure 4.2. *Images of the molecules along the scratched surface with TEFLON. On the left it shows two different areas of the sample. The red arrow represents the direction of the scratch. On the right, they are represented the groups of molecules which follow the same direction (green arrows).*

For each molecule was obtained the same data than in the previous section (FWHM, angle, intensity, ratio…). The goal of this experience is to compare the orientation of the molecules with the orientation of the scratches. For this, it was compared the angle of each molecule with the angle of the green arrow as showed in figure 4.2 depending on the interval along the PTFE molecules where the molecule pertain. The results of this analysis are shown in the figure 4.3. The angle distribution of the analyzed molecules presents a peak at about 10° respect the ideal case (0° difference angle Alexa molecule - angle PTFE molecule). About 60% of the molecules display a deviation from the orientation of the PTFE structure of only 10°.

In this way, we have checked that our approach is working correctly and we can study the orientation of the molecules without using the defocus imaging. Furthermore, we have proved molecules are oriented along the direction of the scratch done in the surface.

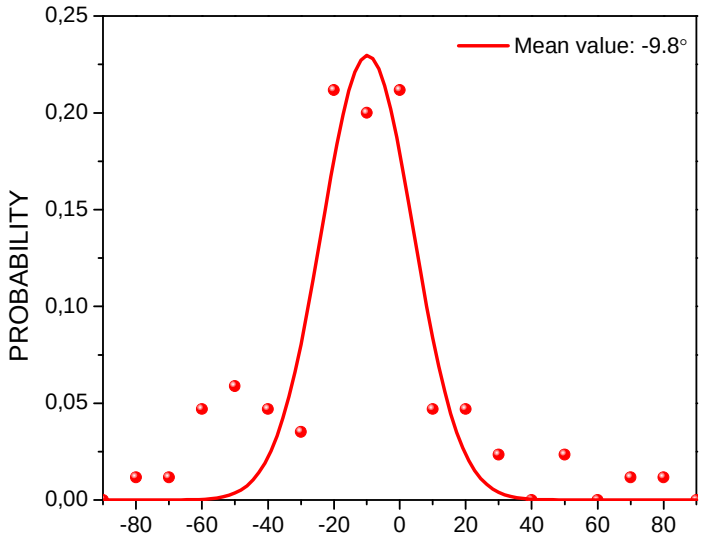

Figure 4.3. *Relation between molecules angle and the scratch angle.*

Another interesting result we obtained in these measurements was the ratio value. As it was said, the ratio tells us if molecules being analyzed are in the correct focal position. The ratio value obtained from this analysis was 1.35, and is the ideal value predicted by the theory. This value has improved respect to the value obtained in the previous section. This is because of these measurements were done in the last period and we had more practise in the making measures. For that reason, the focal position was better determined and the ratio was better. The distribution of the ratio of the molecules studied in this experience is shown in figure 4.4. Thanks to the analysis made earlier we know that this number is remarkably close to the ideal case suggesting our improvement in the experimental protocol.

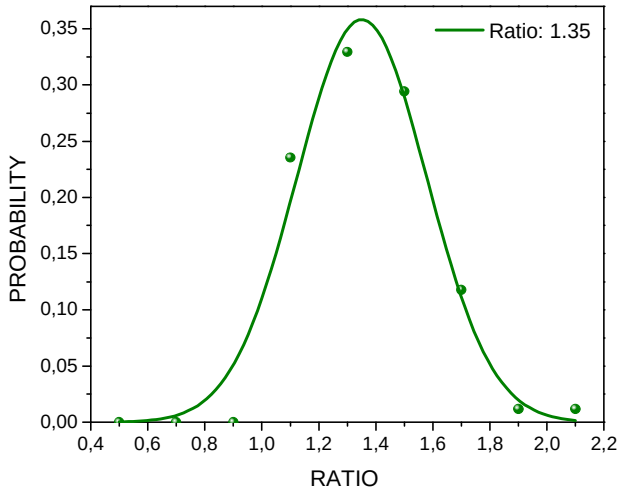

Figure 4.4*. Ratio distribution of the Alexa molecules distribute above a surface scratched with Teflon.*

5. CONCLUSIONS.

The main goal of this project was to verify that the measurement of position and orientation of single molecules could be carried out, with the help of our method, in a simpler, faster and still equally accurate way if compared to the approaches used so far. We fully achieved our goal.

In the first part of this paper, it was explained how the PSF becomes elliptical increasing the collection angle. To get this behaviour two different conditions have to be taken in account: i) the collection angle has to be big enough to appreciate the elliptical shape and ii) the emitted light from the source has to be linearly polarized. To get this second condition, Alexa Fluor 488 molecules were fixed with a matrix polymer (PMMA). The objective used for the experiment provides us a 70º collection angle. With these conditions we are able to measure the orientation of a molecule when it is imaged in the focal position.

Measurements were done with two different approaches (focus and defocus imaging) to compare the angle solutions obtained with each one. Data were fitted in a correlation graph where the angle accuracy for 40 nm pixel size was 5º. The achieved accuracy in the position measurement is about 1.5 nm.

Thanks to the simulated analysis performed, it was shown how it is possible to further improve the angle accuracy by imaging the molecules using a different magnification. These results are shown in the focus-defocus correlation graphs depending on the pixel size. The best precision it was achieved with 80 nm pixel size. This precision was about 5º.

With these results we can conclude that our approach works correctly and we have proved the correlation of the angle's value focus and defocus.

An example of the proper functioning of our technique is reflected in the application experiment. This experiment was to study the behaviour of Alexa molecules in presence of pre-oriented structures such as stretched PTFE molecules. For this, we use a Teflon bar to scratch a slide surface and we deposited on it a small concentration of Alexa molecules in PMMA. We used our approach to determinate the position and the orientation of the molecules. We could determine the anisotropic feature of Teflon stretched molecules and not only that; we were able to observe how our molecules were aligned in the same direction than PTFE molecules.

This leaves more questions to ask, but answers to these questions are beyond the scope of this document.

ANNEX

A) Experimental setup.

The images below show the experimental setup used for this project. In the pictures is represented the optical path followed by the laser (blue line) as well as the names of the different apparatus (figure 1).

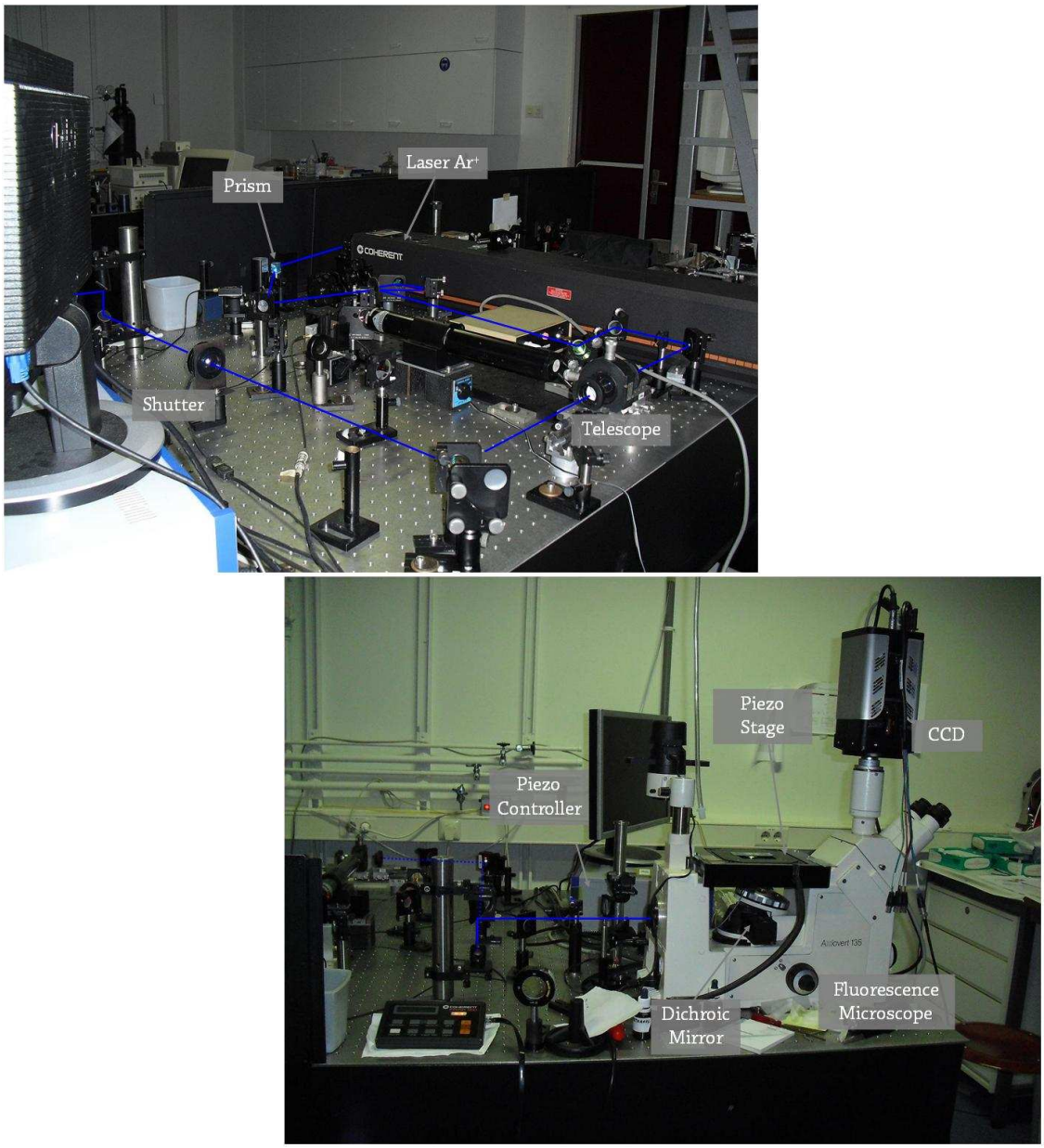

Figure 1. *Experimental setup.*

Light coming out from the laser passes through the prism. Depending on the intensity selected for the laser, we have several slightly shifted wavelengths. With the help of the prism we can spatially separate the different wavelengths and select the proper one. Once we have the desired λ, the light is directed into the telescope by various mirrors.

The role of the telescope is to ensure that the sample is illuminated with homogeneous intensity over its entire surface. The laser beam is a Gaussian beam, i.e., the intensity is much higher in the center of the beam than in the edges (figure 2, a). The telescope achieves that this intensity distribution is wider. In this way, as it was explained in section 2.3, the intensity distribution that passes into the microscope has a difference of 10% of intensity between the centre and the edges of the illuminated area (figure 2, b).

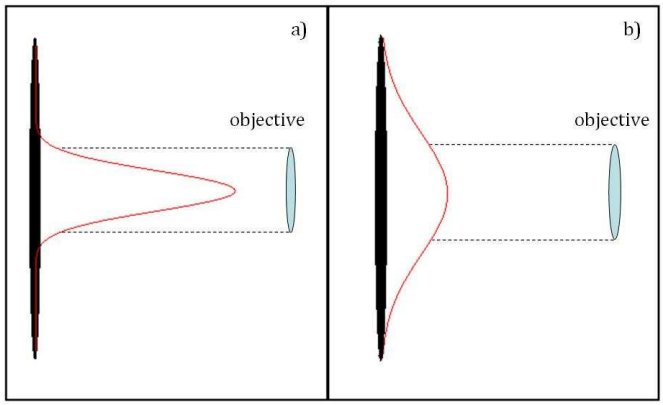

Figure 2. *Laser intensity distribution before and after passing through the telescope*

After the telescope is placed a mechanical shutter (manually controlled) in which the beam stops to avoid the rapid photobleaching of the molecules. Once the beam enters the microscope, the route that follows is the one which was carefully explained in section 2.3.

Photons emitted (fluorescence) by the molecule are collected by the CCD (charge-coupled device) camera. This camera transforms the photons into the electronic signal afterwards processed by the computer or we can observe them directly through the ocular. CCD camera provides digital images of the molecules which are analyzed later.

Two piezo stages are used to control the x, y, and z positioning. One controlling the z position and on which the objective is mounted, and a second piezo stage for the x and y position of the sample.

ACKNOWLEDGMENTS

This project has been one of the most rewarding experiences of my academic life; not only because of the work I did, but also because of the people I worked with. I am deeply grateful to the OCMP group (University of Groningen) for their warm welcome and the fantastic treatment they gave me.

I want to thank Prof. Dr. Ir. Paul H. M. van Loosdrecht for giving me the opportunity to join to this group as well as the confidence and support he has placed in me. I also want to thank Dr. Maxim S. Pchenitchnikov for the time spent working with me on the project and his endeavor in pushing me to produce my best work. Thank you both for the explanations and the discussions accomplished during these months. I really learnt a lot.

I would like to give a special mention to my mentor in this project, Filippo Lusitani. I am extremely grateful for the time you spent teaching and showing me all the things related with this project. I learnt how to work in the laboratory and in the university environment. Thank you for those long talks in the office and all the funny moments we had. You have helped me to grow up as physicist and as person. I was lucky to have you as my mentor.

I also want to thank Foppe de Haan for the help provided. His mathematical and informatics knowledge facilitated my work a great deal. Thanks Foppe for your great patience and your excellent work.

Personally, I would like to thank my family for the support shown in every moment. Without their help I would not have been able to make this dream come true.

REFERENCES

[1] F. Ritort (2006). “Single-molecule experiments in biological physics: methods and applications” PACS number: 82.35.-x, 82.37.-j, 87.15.-v.

[2]Erdal Toprak, J. E., Sheyum Syed, Sean A. McKinney, Rolfe G. Petscheck, Taekjip Ha, Yale E. Goldman, and Paul R. Selvin (2006). "Defocused orientation and position imaging (DOPI) of myosin V." PNAS **103**(17): 6495-6499.

[3] F. Aguet, S. Geissb¨uhler, I. M¨arki, T. Lasser and Michael Unser, “Super-resolution orientation estimation and localization of fluorescent dipoles using 3-D steerable filters” Optics express **17**(8): 6829-6848.

[4] Sri Rama Prasanna Pavani, Michael A. Thompson, Julie S. Biteen, Samuel J. Lord, Na Liu, Robert J. Twieg, Rafael Piestun and W.E. Moerner (2009) “Three-dimensional, single-molecule fluorescence imaging beyond the difrfraction limit by using a double-helix point spread function” PNAS **106**(9): 2995-2999.

[5] P. Lemmer, M. Gunke. D. Baddeley, R. Kaufmann, A. Urich, . Wieland, J. Reymann, P. Müller, M. Hausmann, C. Cremer (2008) “SPDM: light microscopy with single-molecule resolution at the nanoscale” APPLIED PHYSICS B: LASERS AND OPTICS. Vol. 93, Nr. 1, 1-12, DOI: 10.1007/s00340-008-3152-x

[6] Eric M Phizicky and Stanley Fields (1995). “Protein-Protein Interactions:Methods for Detection and Analysis” Microbiological reviews. Vol.59, No. 1, p.94-123

[7] J.R. Lundblad, M Laurence and R. H. Goodman (1996) “Fluorescence polarization analysis of protein-DNA and protein-protein interactions” Molecular endocrinology **10**(6): 607-612.

[8] JR Lakowicz, “Principles of Fluorescence Spectroscopy” Third edition (September 15, 2006)

[9] Lorette C. Javois “Immunothytochemical methods and protocols” Methods in molecular biology **115**

[10] M. Bohmer and J. Enderlein. “Orientation imaging of single molecules by wide-field epifluorescence microscopy”. Optical Society of America **20**(3).

[11] Russell E. Thompson, D. R. L., and Watt W. Webb (2002). "Precise Nanometer Localization Analysis for Individual Fluorescent Probes." Biophysical Journal **82**: 2775-2783.

[12] Wolf, B. R. a. E. (1959). "Electromagnetic Diffraction in Optical Systems. II. Structure of the Image Field in an Aplanatic System." The Royal Society **253**(1274): 358 - 379.

[13] Gill R. E. Design, synthesis and characterization of luminescent organic semiconductors. Phd Thesis, Rijksunivesiteit Groningen, Groningen, 1996.